Inorg. Chem. **2006**, *45*, 2430–2437

Inorganic Chemistry
Article

Influence of Water Content on the Self-Assembly of Metal–Organic Frameworks Based on Pyridine-3,5-dicarboxylate

Yi-Long Lu,[†,‡] Jing-Yun Wu,[†] Ming-Che Chan,[†,§] Sheng-Ming Huang,[#] Chia-Shiang Lin,[⊥] Te-Wei Chiu,[†] Yen-Hsiang Liu,[†] Yuh-Sheng Wen,[†] Chuen-Her Ueng,[⊥] Tsung-Mei Chin,[#] Chen-Hsiung Hung,*[,‡] and Kuang-Lieh Lu*[,†]

Institute of Chemistry, Academia Sinica, Taipei 115, Taiwan, Department of Chemistry, National Changhua University of Education, Changhua 500, Taiwan, Department of Chemistry and Biochemistry, National Chung Cheng University, Chia-Yi 621, Taiwan, Department of Chemistry, Chinese Culture University, Taipei 111, Taiwan, and Department of Chemistry, National Taiwan Normal University, Taipei 106, Taiwan

Received July 27, 2005

A 0D discrete molecule $[Co(3,5\text{-pdc})(H_2O)_5]\cdot 2H_2O$ (**1**) was obtained in quantitative yield from the reaction of $CoCl_2\cdot 6H_2O$ and pyridine-3,5-dicarboxylate (3,5-pdc) in pure water solvent at ambient temperature. While a 1D zigzag chain species, $[\{Co(3,5\text{-pdc})(H_2O)_4\}\cdot H_2O]_n$ (**2**), was produced in a water-rich environment, a 2D layer compound, $[Co(3,5\text{-pdc})(H_2O)_2]_n$ (**3**), with a 6^3 topology was generated under a water-reduced condition and a 2D sheet structure, $[\{Cu(3,5\text{-pdc})(py)_2\}\cdot H_2O\cdot EtOH]_n$ (**4**), was formed under a water-poor condition. Compounds **1**, **2**, and **4** were characterized by single-crystal X-ray diffraction analysis. The 1D zigzag chain **2** shows a recoverable collapsing property. Compound **4** adopts a 2D sheet structure with a $4\cdot 8^2$ topology, observed for the first time for the 3,5-pdc-related metal–organic frameworks. Water content was found to be an important factor in determining the topologies of the products in the self-assembly of divalent metal ions (Co^{2+}, Cu^{2+}) and pyridine-3,5-dicarboxylate under mild conditions.

Introduction

Although the self-assembly of extended organic/inorganic hybrid frameworks has been the subject of extensive study over the years,[1−3] the controlling factors and the experimental conditions for the preparation of functional materials are not completely understood. The design and utilization of molecular building units that contain "preprogrammed" structural information and functionality promises to offer an efficient solution to this challenging problem.[4,5] On the basis of metal−carboxylate cluster ($M_x(O_2C-)_y$) building units, robust, thermally stable polymeric networks with large pores have been generated.[3,5,6] However, the control of the orientation and stereochemistry of the building units in the solid-state continue to be an obstacle in the preparation of a given molecular topology and architecture.

---

* To whom correspondence should be addressed. Fax: +886-2-27831237. E-mail: lu@chem.sinica.edu.tw (K.-L.L.).

[†] Academia Sinica.

[‡] National Changhua University of Education.

[§] National Chung Cheng University.

[#] Chinese Culture University.

[⊥] National Taiwan Normal University.

(1) (a) Lehn, J.-M.; Atwood, J. L.; Davies, J. E. D.; MacNicol, D. D.; Vögtle, F. *Comprehensive Supramolecular Chemistry*; Pergamon: Oxford, U.K., 1996. (b) Batten, S. R.; Robson, R. *Angew. Chem., Int. Ed.* **1998**, *37*, 1460. (c) Moulton, B.; Zaworotko, M. J. *Chem. Rev.* **2001**, *101*, 1629. (d) Swiegers, G. F.; Malefetse, T. J. *Chem. Rev.* **2000**, *100*, 3483. (e) Hosseini, M. W. *Acc. Chem. Res.* **2005**, *38*, 313. (f) Feng, S.; Xu, R. *Acc. Chem. Res.* **2001**, *34*, 239.

(2) (a) Long, D.-L.; Hill, R. J.; Blake, A. J.; Champness, N. R.; Hubberstey, P.; Proserpio, D. M.; Wilson, C.; Schröder, M. *Angew. Chem., Int. Ed.* **2004**, *43*, 1851. (b) Ngo, H. L.; Lin, W. *J. Am. Chem. Soc.* **2002**, *124*, 14298. (c) Tong, M.-L.; Chen, X.-M.; Ye, B.-H.; Ji, L.-N. *Angew. Chem., Int. Ed. Engl.* **1999**, *38*, 2237. (d) Jiang, Y.-C.; Wang, S.-L.; Lee, S.-F.; Lii, K.-H. *Inorg. Chem.* **2003**, *42*, 6154. (e) Yeh, T.-T.; Wu, J.-Y.; Wen, Y.-S.; Liu, Y.-H.; Twu, J.; Tao, Y.-T.; Lu, K.-L. *Dalton Trans.* **2005**, 656.

(3) (a) Férey, G. *Science* **2001**, *291*, 994. (b) Bradshaw, D.; Claridge, J. B.; Cussen, E. J.; Prior, T. J.; Rosseinsky, M. J. *Acc. Chem. Res.* **2005**, *38*, 273. (c) Yaghi, O. M.; O'Keeffe, M.; Ockwig, N. W.; Chae, H. K.; Eddaoudi, M.; Kim, J. *Nature* **2003**, *423*, 705. (d) Eddaoudi, M.; Moler, D. B.; Li, H.; Chen, B.; Reineke, T. M.; O'Keeffe, M.; Yaghi, O. M. *Acc. Chem. Res.* **2001**, *34*, 319. (e) Kitaura, R.; Onoyama, G.; Sakamoto, H.; Matsuda, R.; Noro, S.-i.; Kitagawa, S. *Angew. Chem., Int. Ed.* **2004**, *43*, 2684. (f) Dong, Y.-B.; Smith, M. D.; zur Loye, H.-C. *Angew. Chem., Int. Ed.* **2000**, *39*, 4271. (g) Carlucci, L.; Ciani, G.; Proserpio, D. M.; Rizzato, S. *Chem.—Eur. J.* **2002**, *8*, 1519. (h) Rao, C. N. R.; Natarajan, S.; Vaidhyanathan, R. *Angew. Chem., Int. Ed.* **2004**, *43*, 1466.

(4) (a) Lehn, J.-M. *Science* **2002**, *295*, 2400. (b) Lehn, J.-M. *Proc. Natl. Acad. Sci. U.S.A.* **2002**, *99*, 4763.

10.1021/ic0512577 CCC: $33.50

Water is an important medium in enzymatic processes. For example, it is a key participant in the oxygenation chemistry of enzymes.[7−9] A deficiency of water can cause serious problems in a biological system. The nonflammable and nontoxic nature of water supports milder, safer, and more environmentally friendly reaction conditions than traditional organic solvents.[10] Although solvent effects are important factors in determining the frameworks of coordination polymers[11] and in affecting the shape, size, and phase formation of mineral modification,[12] the effect of water content on the self-assembly of supramolecular entities has been addressed to a lesser extent.[13,14] Some recent investigations reported that the composition of reaction media features some interesting results.[7,12,15] For example, the diverse geometries of carboxylate-rich diiron units could be accommodated depending on the amount of water available,[7] and the selective synthesis of orthorhombic and hexagonal phases of $CeOHCO_3$, as well as cubic CeO_2 crystals, are found to be strongly dependent on the ethanol/water ratio in the system.[12] We report herein on the influence of water content on the topologies of metal−organic networks that are self-assembled from pyridine-3,5-dicarboxylate (3,5-pdc) and divalent metal ions (Co^{2+}, Cu^{2+}) under mild conditions.

Experimental Section

Materials and Instruments. Chemical reagents and solvents were purchased commercially and were used as received without further purification. Thermogravimetric (TG) analyses were performed under nitrogen with a Perkin-Elmer TGA-7 TG analyzer. Elemental analyses were conducted on a Perkin-Elmer 2400 CHN elemental analyzer. Powder X-ray diffraction (PXRD) data were recorded on a Siemens D5000 diffractometer at 40 kV, 30 mA for Cu Kα ($\lambda = 1.5406$ Å), with a step size of 0.02° in θ and a scan speed of 1 s per step size.

Synthesis of $[Co(3,5\text{-}pdc)(H_2O)_5]\cdot 2H_2O$ (1). $CoCl_2\cdot 6H_2O$ (0.30 mmol), 3,5-H_2pdc (0.30 mmol), and KOH (0.30 mmol) were dissolved in 20 mL of H_2O. The aqueous solution was then stirred for 0.5 h at room temperature. After the solution was allowed to stand for 1 day, orange crystals of $[Co(3,5\text{-}pdc)(H_2O)_5]\cdot 2H_2O$ (**1**) were obtained in a quantitative yield. Anal. Calcd for $C_7H_{17}CoNO_{11}$: C, 24.01; H, 4.89; N, 4.00. Found: C, 23.41; H, 4.35; N, 3.87.

Synthesis of $[\{Co(3,5\text{-}pdc)(H_2O)_4\}\cdot H_2O]_n$ (2) and $[Co(3,5\text{-}pdc)(H_2O)_2]_n$ (3). A solution of $CoCl_2\cdot 6H_2O$ (0.20 mmol) in EtOH (95%, 2 mL) was slowly layered on the top of a mixture of EtOH and H_2O (1:5, middle), and an aqueous solution (2 mL, bottom) of 3,5-H_2pdc (0.20 mmol) and KOH (0.50 mmol) at room temperature. Orange crystals of $[\{Co(3,5\text{-}pdc)(H_2O)_4\}\cdot H_2O]_n$ (**2**, 61% yield, major product) and pink crystals of $[Co(3,5\text{-}pdc)(H_2O)_2]_n$ (**3**, 12%, minor product) were obtained after approximately a week. Anal. Calcd for $C_7H_{13}CoNO_9$ (**2**): C, 26.75; H, 4.17; N, 4.46. Found: C, 26.44; H, 3.94; N, 3.97.

Controlled Self-Assembly of $[\{Co(3,5\text{-}pdc)(H_2O)_4\}\cdot H_2O]_n$ (2) and $[Co(3,5\text{-}pdc)(H_2O)_2]_n$ (3). Fine-tuning of the water content in self-assembly reaction systems was found to be an effective technique for controlling the ratio of products $[\{Co(3,5\text{-}pdc)(H_2O)_4\}\cdot H_2O]_n$ (**2**) and $[Co(3,5\text{-}pdc)(H_2O)_2]_n$ (**3**). Orange crystals of **2** could be obtained without the presence of **3** by carefully layering an ethanolic solution of $CoCl_2\cdot 6H_2O$ on the top of an aqueous solution of 3,5-H_2pdc and KOH. On the other hand, if an ethanolic solution of $CoCl_2\cdot 6H_2O$ was carefully layered on the top of a solution of 3,5-H_2pdc and KOH in ethylene glycol and EtOH, pink crystals of **3** were produced in the absence of compound **2**.

Synthesis of $[\{Cu(3,5\text{-}pdc)(py)_2\}\cdot H_2O\cdot EtOH]_n$ (4). A solution of $Cu(NO_3)_2\cdot 3H_2O$ (1.01 mmol) in EtOH (95%, 20 mL) was slowly layered on top of a solution of 3,5-H_2pdc (1.01 mmol) in benzene (20 mL) and pyridine (py, 1 mL) at room temperature. The resulting blue crystals **4** were isolated in a 33% yield (based on the copper) after 10 days. Anal. Calcd for $C_{19}H_{21}CuN_3O_6$: C, 50.61; H, 4.69; N, 9.32. Found: C, 50.47; H, 4.48; N, 9.49.

Crystallographic Determination. Suitable single crystals of **1**, **2**, and **4** were selected for indexing and the collection of intensity data. Measurements were performed using graphite-monochromatized Mo Kα radiation ($\lambda = 0.71073$ Å) on a Siemens P4 diffractometer for **1**, on an Enraf-Nonius CAD4 diffractometer for **2**, and on a Bruker SMART CCD 1000 diffractometer for **4**. Intensity data for **1**, **2**, and **4** were collected at 153(2), 293(2), and 273(2) K, respectively, with the $\omega-2\theta$ scan method. Direct methods were used to solve the structures of compounds **1**, **2**, and **4** using the WINGX[16] and SHELX-97[17] program packages. Structural refinements were done by the full-matrix least-squares method on F^2. All non-hydrogen atoms were refined anisotropically. All of the C−H hydrogen atoms of the guest solvents in **4** and the aromatic C−H hydrogen atoms in **1**, **2**, and **4** were assigned by geometrical calculation. Experimental details for X-ray data collection and the refinements of **1**, **2**, and **4** are given in Table 1.

Results and Discussion

Synthesis and Structural Description. Reaction of $CoCl_2\cdot 6H_2O$ with pyridine-3,5-dicarboxylic acid (3,5-H_2pdc)

---

(5) (a) Abrahams, B. F.; Moylan, M.; Orchard, S. D.; Robson, R. *Angew. Chem., Int. Ed.* **2003**, *42*, 1848. (b) Seo, J. S.; Whang, D.; Lee, H.; Jun, S. I.; Oh, J.; Jeon, Y. J.; Kim, K. *Nature* **2000**, *404*, 982. (b) Chui, S. S.-Y.; Lo, S. M.-F.; Charmant, J. P. H.; Orpen, A. G.; Williams, I. D. *Science* **1999**, *283*, 1148. (c) Holiday, B. J.; Mirkin, C. A. *Angew. Chem., Int. Ed.* **2001**, *40*, 2022. (d) Lu, K.-L.; Chen, Y.-F.; Liu, Y.-H.; Cheng, Y.-W.; Liao, R.-T.; Wen, Y.-S. *Cryst. Growth Des.* **2005**, *5*, 403. (e) Liu, Y.-H.; Wu, H.-C.; Lin, H.-M.; Hou, W.-H.; Lu, K.-L. *Chem. Commun.* **2003**, 60.

(6) (a) Zhao, B.; Yi, L.; Dai, Y.; Chen, X.-Y.; Cheng, P.; Liao, D.-Z.; Yan, S.-P.; Jiang, Z.-H. *Inorg. Chem.* **2005**, *44*, 911. (b) de Lill, D. T.; Gunning, N. S.; Cahill, C. L. *Inorg. Chem.* **2005**, *44*, 258. (c) Zheng, X.; Sun, C.; Lu, S.; Liao, F.; Gao, S.; Jin, L. *Eur. J. Inorg. Chem.* **2004**, 3262. (d) Pan, L.; Woodlock, E. B.; Wang, X.; Zheng, C. *Inorg. Chem.* **2000**, *39*, 4174. (e) Liu, Y.-H.; Lu, Y.-L.; Wu, H.-C.; Wang, J.-C.; Lu, K.-L. *Inorg. Chem.* **2002**, *41*, 2592.

(7) Yoon, S.; Lippard, S. J. *J. Am. Chem. Soc.* **2004**, *126*, 16692.

(8) Wallar, B. J.; Lipscomb, J. D. *Chem. Rev.* **1996**, *96*, 2625.

(9) (a) Gherman, B. F.; Dunietz, B. D.; Whittington, D. A.; Lippard, S. J.; Friesner, R. A. *J. Am. Chem. Soc.* **2001**, *123*, 3836. (b) Gherman, B. F.; Baik, M.-H.; Lippard, S. J.; Friesner, R. A. *J. Am. Chem. Soc.* **2004**, *126*, 2978.

(10) (a) Manabe, K.; Kobayashi, S. *Chem.*−*Eur. J.* **2002**, *8*, 4094. (b) Chatterjee, A.; Maiti, D. K.; Bhattacharya, P. K. *Org. Lett.* **2003**, *5*, 3967. (c) Ma, Y.; Liu, H.; Chen, L.; Cui, X.; Zhu, J.; Deng, J. *Org. Lett.* **2003**, *5*, 2103. (d) Takami, K.; Yorimitsu, H.; Shinokubo, H.; Matsubara, S.; Oshima, K. *Org. Lett.* **2001**, *3*, 1997. (e) Shie, J.-J.; Fang, J.-M. *J. Org. Chem.* **2003**, *68*, 1158.

(11) (a) Lee, I. S.; Shin, D. M.; Chung, Y. K. *Chem.*−*Eur. J.* **2004**, *10*, 3158. (b) Hannon, M. J.; Painting, C. L.; Plummer, E. A.; Childs, L. J.; Alcock, N. W. *Chem.*−*Eur. J.* **2002**, *8*, 2225.

(12) Chen, S.; Yu, S.-H.; Yu, B.; Ren, L.; Yao, W.; Cölfen, H. *Chem.*−*Eur. J.* **2004**, *10*, 3050.

(13) Hagen, K. S.; Lachicotte, R. *J. Am. Chem. Soc.* **1992**, *114*, 8741.

(14) Coucouvanis, D.; Reynolds, R. A., III; Dunham, W. R. *J. Am. Chem. Soc.* **1995**, *117*, 7570.

(15) Tho, I.; Kjøniksen, A.-L.; Nyström, B.; Roots, J. *Biomacromolecules* **2003**, *4*, 1623.

(16) Farrugia, L. J. *J. Appl. Crystallogr.* **1999**, *32*, 837.

(17) Sheldrick, G. M. *SHELX-97*; University of Göttingen: Göttingen, Germany, 1997.

Table 1. Crystal Data and Structure Refinements for **1**, **2**, and **4**

	1	**2**	**4**
empirical formula	$C_7H_{17}CoNO_{11}$	$C_7H_{13}CoNO_9$	$C_{19}H_{21}CuN_3O_6$
fw	350.15	314.11	450.93
cryst syst	orthorhombic	monoclinic	monoclinic
space group	$Cmc2_1$	$P2_1/c$	$P2_1/n$
a (Å)	11.725(2)	11.389(2)	8.7642(16)
b (Å)	15.846(3)	7.1010(14)	19.750(3)
c (Å)	6.9780(14)	15.687(3)	11.4116(16)
α (deg)	90	90	90
β (deg)	90	116.33(3)	100.492(2)
γ (deg)	90	90	90
V (Å^3)	1296.5(4)	1137.0(4)	1942.24(50)
Z	4	4	4
T (K)	153(2)	293(2)	273(2)
λ (Å)	0.71073	0.71073	0.71073
D_{calcd} (g/cm^3)	1.794	1.835	1.542
μ (mm^{-1})	1.382	1.552	1.167
F(000)	724	644	932
R1[a] [$I > 2\sigma(I)$]	0.0373	0.0289	0.0643
wR2[a] [$I > 2\sigma(I)$]	0.0980	0.0856	0.1751
R1[a] [all data]	0.0410	0.0352	0.0772
wR2[a] [all data]	0.1013	0.0908	0.1819
GOF	1.099	1.029	1.081

[a] $R1 = \sum||F_o| - |F_c||/\sum|F_o|$, $wR2 = [\sum w(F_o^2 - F_c^2)^2/\sum w(F_o^2)^2]^{1/2}$.

Scheme 1

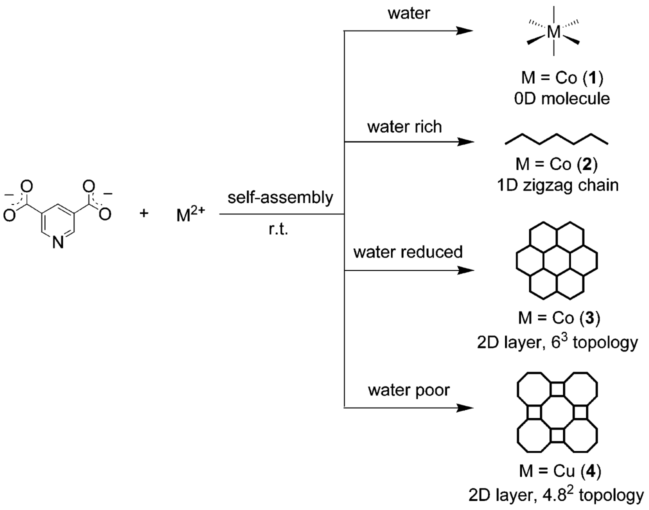

in the presence of KOH in water at ambient temperature led to the formation of $[Co(3,5\text{-pdc})(H_2O)_5]\cdot 2H_2O$ (**1**) in quantitative yield (eq 1, Scheme 1). Structural analysis shows

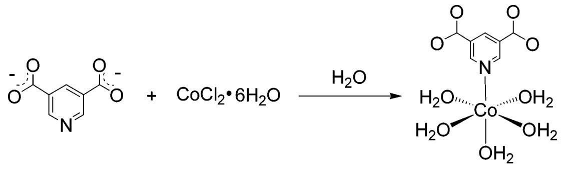

(1)

that **1** is a 0D discrete molecule (Figure 1), in which the Co(II) ion is coordinated by one nitrogen atom from one 3,5-pdc ligand (Co−N = 2.160(4) Å) and five water molecules (Co−O = 2.060(4)−2.120(6) Å, Table 2) to furnish an octahedral geometry. As shown in Figure 2a, the $[Co(3,5\text{-pdc})(H_2O)_5]$ moieties are further connected to each other via hydrogen bonds (O···O = 2.660(8)−2.817(4) Å, O−H···O = 163−167°, Table 3), resulting in 2D layers with a 6^3 topology in the *ab* plane. The hydrogen-bonded 2D layers are packed along the *c* axis in an ABAB order (Figure 2b) and are stabilized by interlayer O−H···O hydrogen-bonding interactions (Table 3).

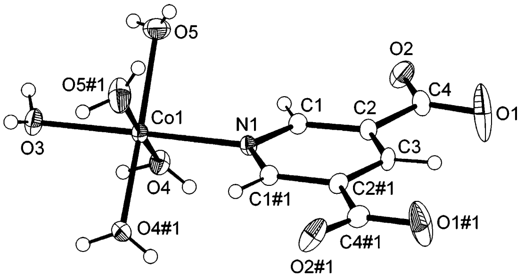

Figure 1. ORTEP diagram of **1** by thermal vibration ellipsoids with a 30% probability level. Uncoordinated water molecules are omitted.

Table 2. Selected Bond Lengths (Å) and Angles (deg) for **1**[a]

Co1−N1	2.160(4)	Co1−O3	2.114(4)
Co1−O4	2.060(4)	Co1−O5	2.120(6)
N1−Co1−O3	179.2(3)	N1−Co1−O4	89.40(14)
N1−Co1−O5	91.16(16)	N1−Co1−O4#1	89.40(14)
N1−Co1−O5#1	91.16(16)	O3−Co1−O4	90.08(14)
O3−Co1−O5	89.41(17)	O3−Co1−O4#1	90.08(14)
O3−Co1−O5#1	89.41(17)	O4−Co1−O5	87.59(18)
O4−Co1−O4#1	95.9(3)	O4−Co1−O5#1	176.4(3)
O5−Co1−O4#1	176.4(3)	O5−Co1−O5#1	88.9(5)
O4#1−Co1−O5#1	87.59(18)		

[a] Symmetry transformations: #1 −*x*, *y*, *z*.

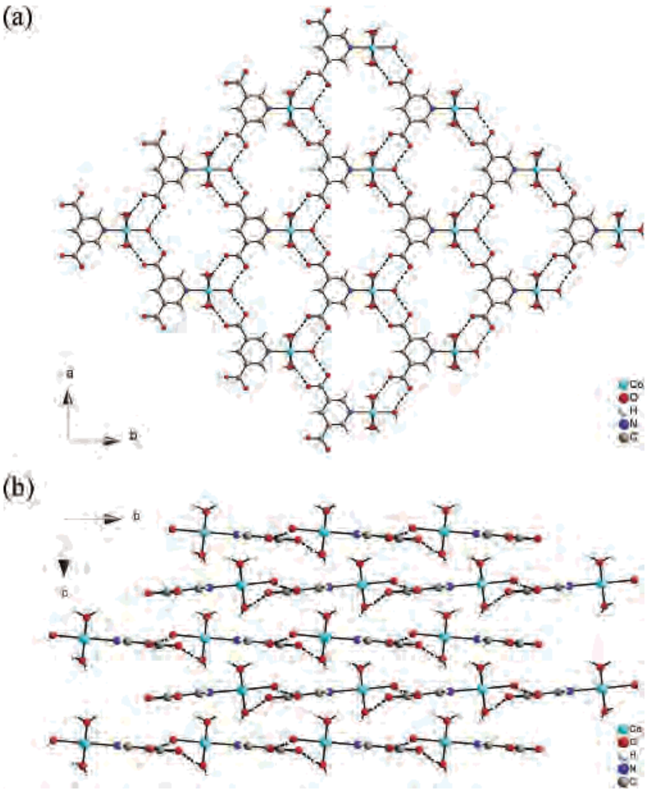

Figure 2. (a) Ball and stick model of **1**, showing the hydrogen-bonded 2D layer architecture with a 6^3 topology in the *ab* plane. (b) Perspective view of the packing diagram of **1**, showing these 2D layers packed along *c* axis in an ABAB order.

The orange crystals of $[\{Co(3,5\text{-pdc})(H_2O)_4\}\cdot H_2O]_n$ (**2**) and the pink crystals of $[Co(3,5\text{-pdc})(H_2O)_2]_n$ (**3**) were obtained by layering an ethanolic solution of $CoCl_2\cdot 6H_2O$ onto an aqueous solution of $3,5\text{-}H_2pdc$ and KOH in the

Table 3. Hydrogen-Bonding Geometry (Å, deg) in **1**[a]

D−H⋯A	*d*(D−H)	*d*(H⋯A)	*d*(D⋯A)	∠D−H⋯A
O3−H3A⋯O2#1	0.82	2.02	2.817(4)	163
O4−H4⋯O2#2	0.82	1.93	2.702(5)	158
O5−H5⋯O1#1	0.82	1.86	2.660(8)	167
O4−H11⋯O6#2	0.74	2.02	2.716(6)	155
O5−H12⋯O6#3	0.65	2.28	2.839(7)	147
O6−H13⋯O5#2	0.91	2.47	2.839(7)	105
O6−H14⋯O1#1	0.63	2.08	2.684(5)	162

[a] Symmetry transformations: #1 1/2 − *x*, 1/2 + *y*, *z*; #2 1/2 − *x*, 1/2 − *y*, − 1/2 + *z*; #3 1/2 − *x*, 1/2 − *y*, 1/2 + *z*.

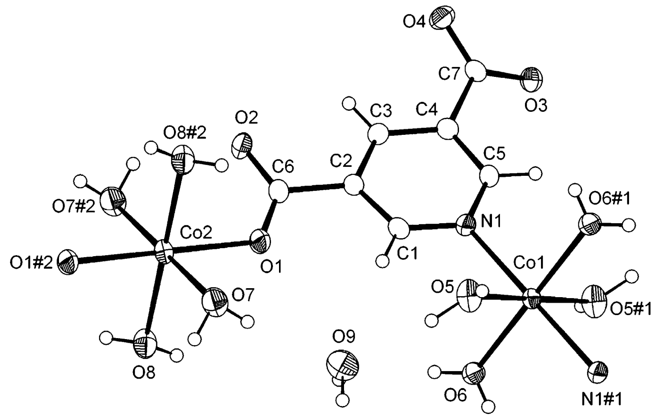

Figure 3. ORTEP diagram of **2** with thermal vibration ellipsoids at the 50% probability level.

Table 4. Selected Bond Lengths (Å) and Angles (deg) for **2**[a]

Co1−N1	2.1688(18)	Co2−O1	2.1020(16)
Co1−O5	2.1372(16)	Co2−O7	2.0827(16)
Co1−O6	2.0364(15)	Co2−O8	2.0841(15)
N1−Co1−O5	88.98(7)	O1−Co2−O7	84.80(7)
N1−Co1−O5#1	91.02(7)	O1−Co2−O7#2	95.20(7)
N1−Co1−O6	89.04(6)	O1−Co2−O8	93.62(6)
N1−Co1−O6#1	90.96(6)	O1−Co2−O8#2	86.38(6)
O5−Co1−O6	90.52(7)	O7−Co2−O8	89.91(6)
O5−Co1−O6#1	89.48(7)	O7−Co2−O8#2	90.09(6)

[a] Symmetry transformations: #1 −*x*, −*y* + 2, −*z*; #2 −*x* + 1, −*y* + 2, −*z* + 1.

presence of a buffer layer of EtOH and H_2O (1:5) at ambient temperature. The formation of compound **2** without **3** could be achieved by using water and ethanol as the solvent pair. On the other hand, when ethylene glycol and ethanol were used as the solvent system, **3** could be obtained without **2**. This indicates that fine-tuning the water content in self-assembly reaction systems is an effective way to control the ratio of products **2** and **3**. The former was obtained as the major product at a higher concentration of water (water-rich conditions), while the latter was the major product when a lower concentration of water (water-reduced conditions) was used (Scheme 1).

A single-crystal X-ray diffraction analysis reveals that **2** adopts a 1D zigzag chain architecture. There are two distinct cobalt ions in the structure of **2** (Figure 3). In addition to four coordinated water molecules (Co−O(water) = 2.0364(15)−2.1372(16) Å, Table 4), Co1 is bound to two pyridyl nitrogen atoms (Co1−N1 = 2.1688(18) Å), while Co2 is bound to two monodentate carboxylate oxygen atoms (Co2−O1 = 2.1020(16) Å) from two distinct 3,5-pdc ligands. On the other hand, each 3,5-pdc ligand is bound to two Co(II) ions through one monodentate carboxylate and one pyridyl group. The packing diagram shows that the 1D zigzag chain is stabilized by numerous hydrogen bonding and $\pi-\pi$ interactions, forming 1D hydrophilic channels along the crystallographic *b* axis with guest water molecules inside (Figure 4). Several types of hydrogen bonds are observed in the structure: (a) coordinated water molecules bonded to noncoordinated carboxylate oxygen atoms (O⋯O distances = 2.654(2)−3.061(3) Å), (b) uncoordinated water molecules bonded to the noncoordinated carboxylate oxygen atoms (O⋯O distances = 2.897(3)−2.899(3) Å), and (c) coordinated water molecules bonded to uncoordinated water molecules (O⋯O distances = 2.854(3)−2.874(3) Å). Detailed data are given in Table 5. The centroid⋯centroid distance for the $\pi-\pi$ interactions between pyridine rings on the adjacent chain is 3.68 Å.

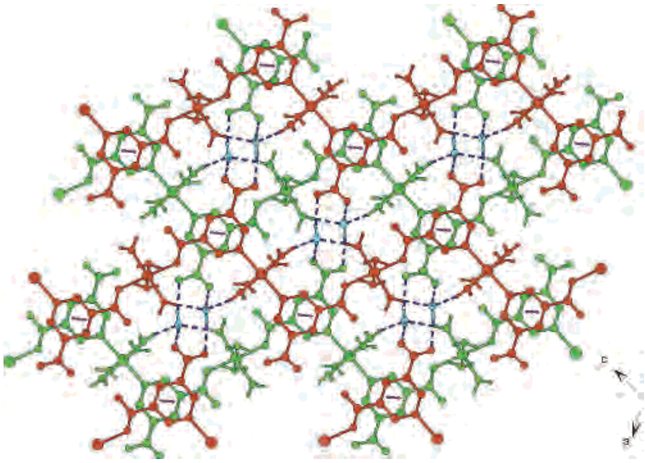

Figure 4. Perspective view of the packing diagram of **2** along the *b* axis, showing 1D hydrophilic channels with guest water molecules inside. The green and orange colors exhibit the 1D zigzag chain structures, the cyan color represents guest water molecules, the blue dashed bonds show the O−H⋯O hydrogen-bonding interactions between the guest water molecules and the 1D zigzag chains, and the purple dashed bonds show the $\pi-\pi$ interactions between two stacked aromatic rings.

Table 5. Hydrogen-Bonding Geometry (Å, deg) in **2**[a]

D−H⋯A	*d*(D−H)	*d*(H⋯A)	*d*(D⋯A)	∠D−H⋯A
O5−H11⋯O(9)#1	0.90(3)	2.00(3)	2.874(3)	166(3)
O5−H12⋯O(2)#2	0.71(4)	2.14(3)	2.839(2)	174(4)
O6−H13⋯O(2)#3	0.73(3)	1.99(3)	2.670(2)	154(3)
O6−H14⋯O(4)#4	0.78(3)	1.89(3)	2.654(2)	167(3)
O7−H15⋯O(9)#1	0.77(3)	2.09(3)	2.854(3)	173(4)
O7−H16⋯O(4)#5	0.90(4)	2.49(3)	3.061(3)	122(2)
O7−H16⋯O(2)#6	0.90(4)	2.19(3)	2.819(3)	127(2)
O8−H17⋯O(3)#4	0.80(3)	1.94(3)	2.734(2)	170(3)
O8−H18⋯O(3)#7	0.86(3)	1.93(3)	2.734(2)	157(3)
O9−H19⋯O(3)#4	0.83(5)	2.08(5)	2.899(3)	166(4)
O9−H20⋯O(4)#8	0.79(4)	2.13(4)	2.897(3)	163(4)

[a] Symmetry transformations: #1 1 − *x*, 1/2 + *y*, 1/2 − *z*; #2 *x*, 5/2 − *y*, −1/2 + *z*; #3 *x*, 3/2 − *y*, −1/2 + *z*; #4 −*x*, −1/2 + *y*, 1/2 − *z*; #5 1 + *x*, *y*, *z*; #6 1 − *x*, 2 − *y*, 1 − *z*; #7, 1 + *x*, 3/2 − *y*, 1/2 + *z*; #8, 1 + *x*, −1 + *y*, *z*.

Compound **3** was characterized as a known compound $[Co(3,5\text{-pdc})(H_2O)_2]_n$ by X-ray structure analysis.[18,19] This species is isomorphous with previously reported Cu and Mn derivatives,[20,21] prepared by a hydrothermal method. All these compounds have high coordination numbers, 7 around the metal center, which likely result from the asymmetric

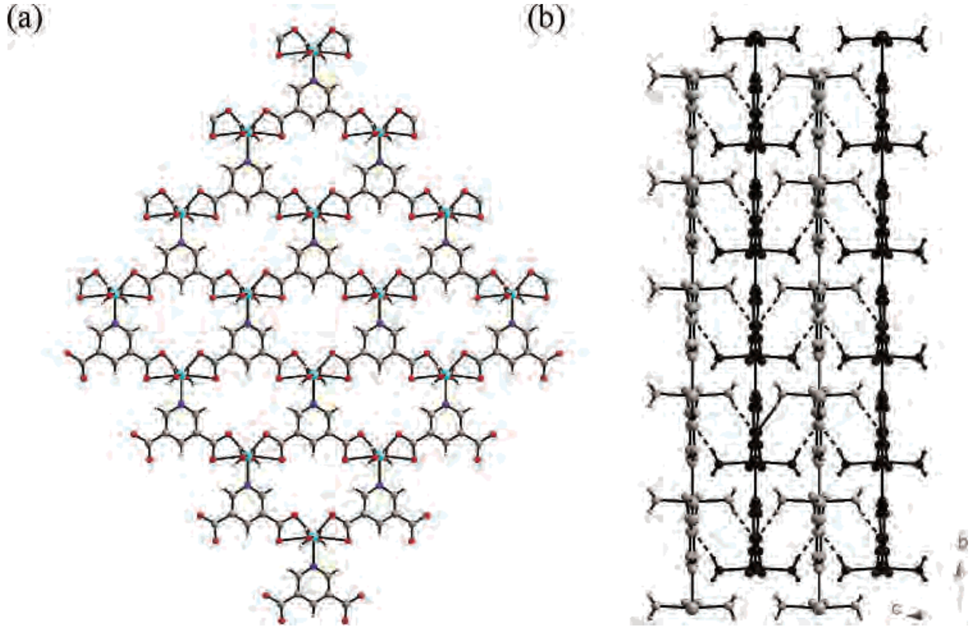

Figure 5. (a) Ball and stick model of **3** at *ab* plane, showing 2D porous sheet architecture with a 6^3 topology. Cyan, Co; red, O; blue, N; medium gray, C; light gray, H. (b) View of the intersheet hydrogen-bonding interactions (dashed bonds) between the axial water molecules and carboxylate groups in **3**.[18,19]

bonding mode of the carboxylate group with different M−O bond lengths.[18−21] Extensive frameworks of these compounds show 2D sheet architecture with 6^3 topology (Figure 5a). Strong intersheet hydrogen-bonding interactions were observed via axial water molecules (Figure 5b).

Compound $[\{Cu(3,5\text{-pdc})(py)_2\}\cdot H_2O\cdot EtOH]_n$ (**4**) was prepared by the slow diffusion of an ethanolic solution of $Cu(NO_3)_2\cdot 3H_2O$ into a benzene solution containing 3,5-H_2pdc and pyridine at room temperature. Blue crystals were produced after ca. 10 days in this water-poor solvent system. A solid-state structure analysis shows that the Cu(II) centers in **4** are coordinated by one monodentate carboxylate, one chelated carboxylate, and one pyridyl nitrogen from three distinct 3,5-pdc ligands and two pyridine molecules (Figure 6). The Cu1−O1 bond is very weak, with a distance of 2.760(3) Å, and can be described as semicoordinated.[23] Therefore the CuN_3O_2 core can be regarded as a square pyramidal geometry. The Cu1−N1(axial) bond with a length of 2.360(3) Å (see Table 6) is longer than the other two equatorial Cu−N bonds (Cu1−N11 = 2.009(2) Å and Cu1−N21 = 2.011(2) Å), indicating the presence of a strong Jahn−Teller effect. The extended structure of **4** exhibits an unprecedented 2D sheet architecture with a $4\cdot 8^2$ topology (Figure 7a).[22] When viewed along the *a* axis, these sheets are stacked eclipsed to govern the framework with hydrophilic channels where the guest water and ethanol molecules reside (Figure 7b). However, the sheets are interleaved with each other and are stabilized by interlayer $\pi-\pi$ interactions between adjacent pyridine molecules.

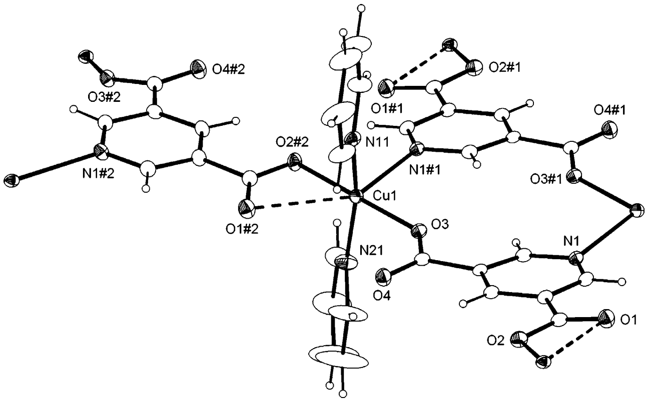

Figure 6. ORTEP drawing of **4** by thermal vibration ellipsoids with 30% probability level. Uncoordinated water and ethanol molecules are omitted.

Table 6. Selected Bond Lengths (Å) and Angles (deg) for **4**[a]

Cu1−O3	1.961(3)	Cu1−N11	2.008(2)
Cu1−O2#2	1.961(3)	Cu1−N21	2.010(2)
Cu1−N1#1	2.361(3)		
O3−Cu1−O2#2	177.76(13)	O2#2−Cu1−N11	89.57(12)
O3−Cu1−N1#1	88.51(12)	O2#2−Cu1−N21	89.13(13)
O3−Cu1−N11	91.90(12)	N1#1−Cu1−N11	95.45(12)
O3−Cu1−N21	89.82(13)	N1#1−Cu1−N21	97.95(13)
O2#2−Cu1−N1#1	89.68(12)	N11−Cu1−N21	166.53(13)

[a] Symmetry transformations: #1 $-x + 1$, $-y$, $-z + 2$; #2 $-x + 1/2$, $y + 1/2$, $-z + 3/2$.

---

(18) Plater, M. J.; Roberts, A. J.; Howie, R. A. *J. Chem. Res. (S)* **1998**, 240.

(19) Whitfield, T.; Zheng, L.-M.; Wang, X.; Jacobson, A. J. *Solid State Sci.* **2001**, *3*, 829.

(20) Lu, J.; Schauss, V. *CrystEngComm* **2001**, *3*, 26.

(21) Xu, H.; Zheng, N.; Xu, H.; Wu, Y.; Yang, R.; Ye, E.; Jin, X. *J. Mol. Struct.* **2002**, *610*, 47.

(22) For examples of some 2D metal−organic frameworks with a $4\cdot 8^2$ topology, see: (a) Barnett, S. A.; Blake, A. J.; Champness, N. R.; Nicolson, J. E. B.; Wilson, C. *J. Chem. Soc., Dalton Trans.* **2001**, 567. (b) Wan, S.-Y.; Fan, J.; Okamura, T.-a.; Zhu, H.-F.; Ouyang, X.-M.; Sun, W.-Y.; Ueyama, N. *Chem. Commun.* **2002**, 2520. (c) Fan, J.; Shu, M.-H.; Okamura, T.-a.; Li, Y.-Z.; Sun, W.-Y.; Tang, W.-X.; Ueyama, N. *New J. Chem.* **2003**, *27*, 1307. (d) Li, C. H.; Si, S. F.; Wang, R. J.; Li, Y. D. *Chin. J. Inorg. Chem.* **2004**, *20*, 536.

(23) (a) Scheidt, W. R.; Lee, Y. J.; Geiger, D. K.; Taylor, K.; Hatano, K. *J. Am. Chem. Soc.* **1982**, *104*, 3367. (b) Hammond, R. P.; Cavaluzzi, M.; Haushalter, R. C.; Zubieta, J. A. *Inorg. Chem.* **1999**, *38*, 1288.

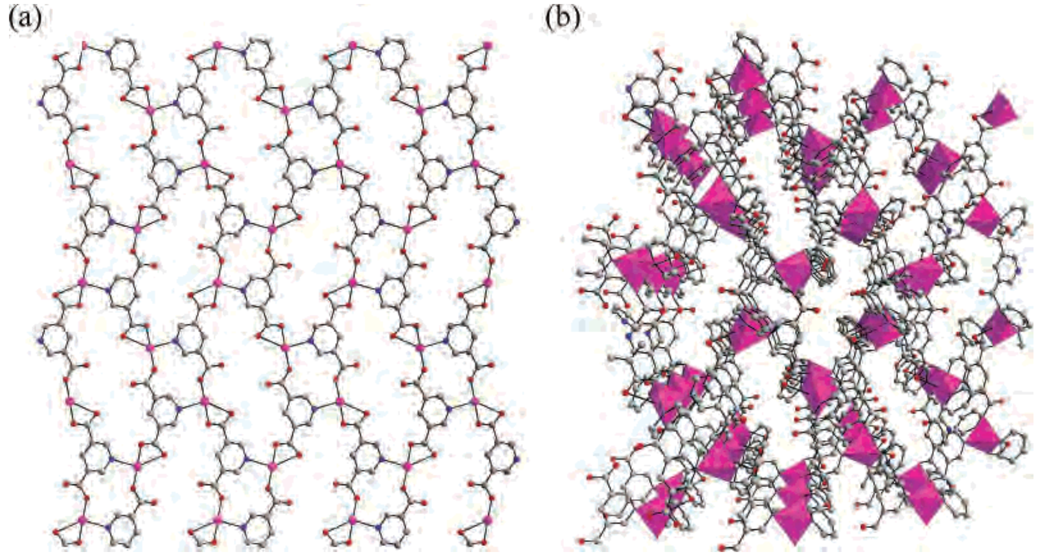

Figure 7. (a) The 2D sheet architecture with a 4·8^2 topology in the *bc* plane in **4**. (b) Perspective view of the framework with the hydrophilic channels of **4** along the *a* axis. Guest molecules, coordination pyridine molecules, and hydrogen atoms are omitted for clarity. Polyhedra, [CuN_3O_3]; pink, Cu; red, O; blue, N; medium gray, C.

Scheme 2

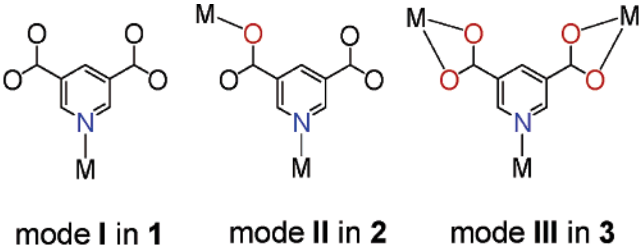

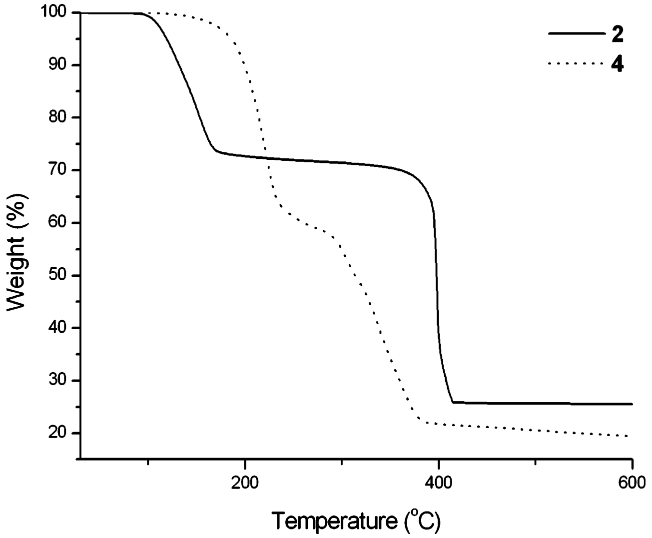

Figure 8. Thermogravimetric analysis (TGA) diagrams of **2** and **4**.

Effect of the Water Content of the Solvent Systems. It is worthwhile to compare the reaction conditions for the self-assembly of divalent metal ions with 3,5-pdc and the architectures of their final products. Pyridine-3,5-dicarboxylate (3,5-pdc) was selected as a building ligand because of its multidentate nature, versatile coordination modes, and sensible correlation of coordination characteristics with reaction parameters. The architectures resulting from the self-assembly of **1**–**4** under mild conditions are strongly influenced by the water content of the solvent systems. The 0D discrete molecule **1** was produced in a pure water environment. The 1D chain structure of **2** was produced in a water-rich environment, while the 2D layer structures of **3** (6^3 topology) and **4** (4·8^2 topology) were generated under water-reduced and water-poor conditions, respectively. The number of coordinated water molecules around the Co(II) center (5 in **1**, 4 in **2**, and 2 in **3**) follows the trend of the gradual reduction of the ratio of water in the solvent systems. This is corroborated by the coordination modes of the 3,5-pdc ligand in compounds **1** (mode **I**), **2** (mode **II**), and **3** (mode **III**, Scheme 2), as a result of the strong competition between the water molecule and the carboxylate group of 3,5-pdc. Thus the water content tunes the coordination environment of the metal centers, leading to the formation of 0D, 1D, and 2D architectures in the products (Scheme 1). Interestingly, compound **4** exhibits an unprecedented two-dimensional 4·8^2 net, different from the commonly observed 6^3 topology in the vast majority of published networks based on 3,5-pdc[18–21]. In addition to the influence of the water-poor condition, the formation of **4** might also be affected by the presence of the pyridine ligand, which donates more electrons to the metal center and influences the asymmetric coordination modes of the carboxylate groups. Finally, it is noteworthy that under hydrothermal conditions, high-dimensional (2D and 3D) networks are preferred for 3,5-pdc-based coordination polymers,[18–21,24,25] even in a pure water medium. This might be attributed to the enhancement of the metal–ligand interactions rather than metal–water coordination under such rigorous conditions.[26] However, under mild conditions, the influence of water content on the self-assembly of supramolecular entities is critical, as revealed by the structural analysis of compounds **1**–**4**. In contrast to compounds **1**–**3**, the formation of **4** is affected

---

(24) Xu, H.; Zheng, N.; Xu, H.; Wu, Y.; Yang, R.; Ye, E.; Jin, X. *J. Mol. Struct.* **2002**, *606*, 117.

(25) Min, D.; Lee, S. W. *Inorg. Chem. Commun.* **2002**, *5*, 978.

(26) Kim, Y. J.; Suh, M.; Jung, D.-Y. *Inorg. Chem.* **2004**, *43*, 245.

Scheme 3

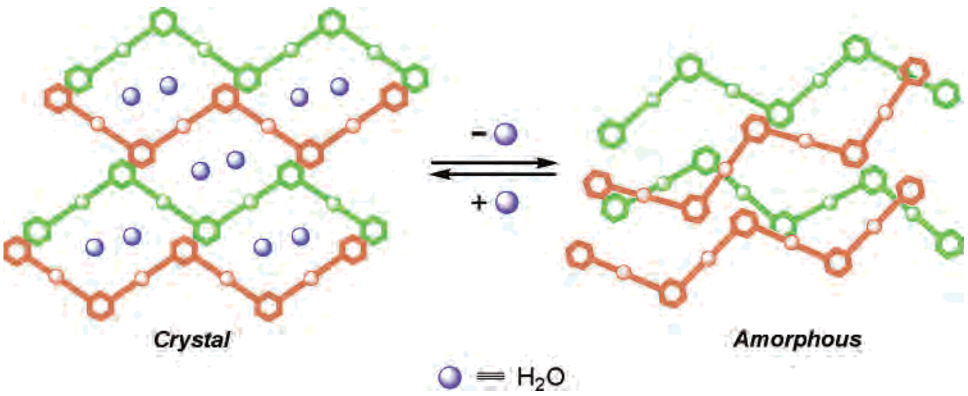

not only by the H_2O content but also by the presence of the pyridine ligand and quite possibly by the fact that **4** contains Cu instead of Co.

Thermogravimetric Analysis (TGA) and X-ray Powder Diffraction (XRPD) Studies. The thermogravimetric analysis of **2**, as shown in Figure 8, shows the release of one guest and four coordinated water molecules between 100 and 175 °C (found, 26.76%; calcd, 28.65%). The percent weight remaining is nearly constant up to 355 °C without any additional weight loss. The TG curve for **4** shows the loss of one guest water molecule, one guest ethanol molecule, and two coordinated pyridine molecules in the temperature range of 128−309 °C (found, 49.17%; calcd, 49.23%). Weight loss occurred gradually up to 390 °C, the decomposition temperature of the compound. The final residual product appears to be CuO, as shown by the 21.92% residue (calcd, 19.65%).

The X-ray powder diffraction (XRPD) patterns for the desorption−sorption studies of **2** are shown in Figure 9. After a fresh sample of **2** was heated to 150 °C, the crystallinity of **2** disappears because of the removal of guest and coordinated water molecules, as confirmed by the flat diffraction pattern (Figure 9c). This is consistent with the TG curve for **2**, in which coordinated water molecules are lost in the temperature range of 100−175 °C (Figure 8). The crystal color changes from pale orange to deep blue on heating. When the heated sample was allowed to naturally cool to room temperature, while exposed to a moist atmosphere for 24 h, the diffraction peaks were recovered (Figure 9d), compared to the original and simulated patterns for **2** (Figures 9a and e), along with the recovery of the crystal color. This indicates that **2** possesses an interesting recoverable collapsing property with the regeneration of crystallinity upon the uptake of guest molecules from the atmosphere (Scheme 3).[27] The property can be attributed to the reformation of the O−H···O hydrogen bonds from guest water molecules to the noncoordinated carboxylate oxygen atoms introduced by the sorption of guest water molecules. Other types of hydrogen bonds (see above structural description for **2**) and the interchain $\pi\cdots\pi$ interactions would then be regenerated through a cooperative assembly process.[28] To the best of our knowledge, compounds showing reversible structural transformations are very rare for 1D coordination polymers,[29] since most examples with reversible crystal-to-amorphous (recoverable collapsing) or crystal-to-crystal (guest-induced reformation) frameworks[27,30] have either 2D or 3D architectures from their stronger network. The recoverable collapsing characteristics with a reversible desorption−sorption property

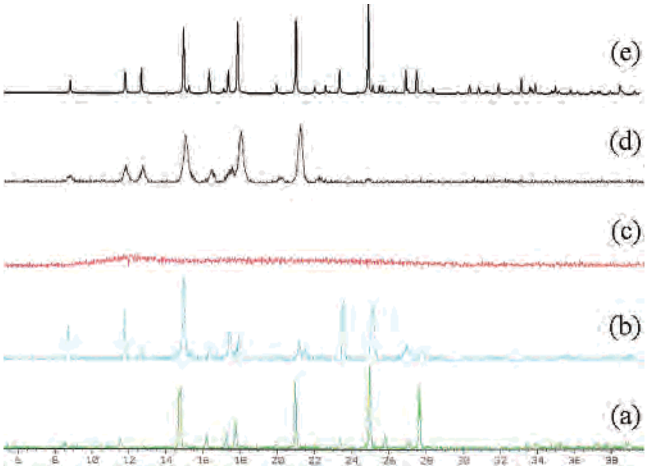

Figure 9. XRPD patterns of **2**: (a) a freshly ground sample at room temperature, (b) after the heating at 100 °C, (c) after the heating at 150 °C, (d) after the exposure of the heated sample to the moist air for 24 h, and (e) simulated from the single-crystal data.

---

(27) (a) Uemura, K.; Kitagawa, S.; Kondo, M.; Fukui, K.; Kitaura, R.; Chang, H.-C.; Mizutani, T. *Chem.—Eur. J.* **2002**, *8*, 3586. (b) Uemura, K.; Kitagawa, S.; Fukui, K.; Saito, K. *J. Am. Chem. Soc.* **2004**, *126*, 3817.

(28) (a) Gong, H.; Krische, M. J. *J. Am. Chem. Soc.* **2005**, *127*, 1719. (b) Thallapally, P. K.; Katz, A. K.; Carrell, H. L.; Desiraju, G. R. *Chem. Commun.* **2002**, 344. (c) Szczesna, B.; Urbañczyk-Lipkowska, Z. *New J. Chem.* **2002**, *26*, 243. (d) Boldog, I.; Rusanov, E. B.; Sieler, J.; Domasevitch, K. V. *New J. Chem.* **2004**, *28*, 756.

(29) (a) Cingolani, A.; Galli, S.; Masciocchi, N.; Pandolfo, L.; Pettinari, C.; Sironi, A. *J. Am. Chem. Soc.* **2005**, *127*, 6144. (b) Yamada, K.; Yagishita, S.; Tanaka, H.; Tohyama, K.; Adachi, K.; Kaizaki, S.; Kumagai, H.; Inoue, K.; Kitaura, R.; Chang, H.-C.; Kitagawa, S.; Kawata, S. *Chem.—Eur. J.* **2004**, *10*, 2647.

(30) (a) Kitaura, R.; Fujimoto, K.; Noro, S.-i.; Kondo, M.; Kitagawa, S. *Angew. Chem., Int. Ed.* **2002**, *41*, 133. (b) Min, K. S.; Suh, M. P. *Chem.—Eur. J.* **2001**, *7*, 303. (c) Choi, H. J.; Lee, T. S.; Suh, M. P. *Angew. Chem., Int. Ed.* **1999**, *38*, 1405. (d) Li, H.; Davis, C. E.; Groy, T. L.; Kelley, D. G.; Yaghi, O. M. *J. Am. Chem. Soc.* **1998**, *120*, 2186. (e) Tabares, L. C.; Navarro, J. A. R.; Salas, J. M. *J. Am. Chem. Soc.* **2001**, *123*, 383. (f) Mäkinen, S. K.; Melcer, N. J.; Parvez, M.; Shimizu, G. K. H. *Chem.—Eur. J.* **2001**, *7*, 5176. (g) Liu, Y.; Su, J.; Li, W.; Wu, J. *Inorg. Chem.* **2005**, *44*, 3890. (h) Pan, L.; Woodlock, E. B.; Wang, X.; Zheng, C. *Inorg. Chem.* **2000**, *39*, 4174. (i) Barea, E.; Navarro, J. A. R.; Salas, J. M.; Masciocchi, N.; Galli, S.; Sironi, A. *J. Am. Chem. Soc.* **2004**, *126*, 3014.

makes the unique 1D compound **2** a potential candidate for application as a good solvent carrier.[27,29−31]

Conclusion

The water content of solvent systems has a significant influence on the structural topologies of the products resulting from the self-assembly of a 3,5-pdc ligand and divalent metal salts under mild conditions. Different from the 6^3 topology of a normal 2D sheet produced from 3,5-pdc and divalent metal ions, a 2D sheet structure, $[\{Cu(3,5\text{-pdc})(py)_2\}\cdot H_2O\cdot EtOH]_n$ (**4**), with a $4\cdot8^2$ topology and a 1D zigzag chain, $[\{Co(3,5\text{-pdc})(H_2O)_4\}\cdot H_2O]_n$ (**2**), with recoverable collapsing properties were obtained. Because of its multidentate nature and its versatile coordination modes, 3,5-pdc appears to be an ideal building unit for use in studies of the correlation of molecular topology with reaction parameters.

Acknowledgment. We thank Academia Sinica and the National Science Council of Taiwan for financial support.

Supporting Information Available: The crystallographic data in CIF format for the structures of **1**, **2**, and **4**. This material is available free of charge via the Internet at http://pubs.acs.org.

IC0512577

---

(31) Kitagawa, S.; Kitaura, R.; Noro, S.-i. *Angew. Chem., Int. Ed.* **2004**, *43*, 2334.